Impact of poloxamer 188 (Pluronic F-68) additive on cell mechanical properties, quantification by real-time deformability cytometry

Impact of poloxamer 188 (Pluronic F-68) additive on cell mechanical properties, quantification by real-time deformability cytometry

Ewa Guzniczak, Melanie Jimenez, Matthew Irwin, Oliver Otto, Nicholas Willoughby, and Helen Bridle

Citation: Biomicrofluidics **12**, 044118 (2018); doi: 10.1063/1.5040316
View online: https://doi.org/10.1063/1.5040316
View Table of Contents: http://aip.scitation.org/toc/bmf/12/4
Published by the American Institute of Physics

Impact of poloxamer 188 (Pluronic F-68) additive on cell mechanical properties, quantification by real-time deformability cytometry

Ewa Guzniczak,[1,a)] Melanie Jimenez,[2] Matthew Irwin,[1] Oliver Otto,[3] Nicholas Willoughby,[1] and Helen Bridle[1]

[1]*Institute of Biological Chemistry, Biophysics and Bioengineering, School of Engineering and Physical Science, Heriot-Watt University, Edinburgh Campus, Edinburgh EH14 4AS, United Kingdom*

[2]*School of Engineering, Biomedical Engineering Division, University of Glasgow, Glasgow G12 8LT, United Kingdom*

[3]*ZIK HIKE, Centre for Innovation Competence - Humoral Immune Reactions in Cardiovascular Diseases, Biomechanics, University of Greifswald, Fleischmannstraße 42-44, 17489 Greifswald, Germany*

(Received 16 May 2018; accepted 3 August 2018; published online 22 August 2018)

Advances in cellular therapies have led to the development of new approaches for cell product purification and formulation, e.g., utilizing cell endogenous properties such as size and deformability as a basis for separation from potentially harmful undesirable by-products. However, commonly used additives such as Pluronic F-68 and other poloxamer macromolecules can change the mechanical properties of cells and consequently alter their processing. In this paper, we quantified the short-term effect of Pluronic F-68 on the mechanotype of three different cell types (Jurkat cells, red blood cells, and human embryonic kidney cells) using real-time deformability cytometry. The impact of the additive concentration was assessed in terms of cell size and deformability. We observed that cells respond progressively to the presence of Pluronic F-68 within first 3 h of incubation and become significantly stiffer (p-value < 0.001) in comparison to a serum-free control and a control containing serum. We also observed that the short-term response manifested as cell stiffening is true (p-value < 0.001) for the concentration reaching 1% (w/v) of the poloxamer additive in tested buffers. Additionally, using flow cytometry, we assessed that changes in cell deformability triggered by addition of Pluronic F-68 are not accompanied by size or viability alterations. *Published by AIP Publishing.* https://doi.org/10.1063/1.5040316

I. INTRODUCTION

The cell therapy market is expected to grow rapidly in the next few decades, leading to an urgent need for new industry compatible cellular processes (Mason *et al.*, 2011; Rao, 2011; Heathman *et al.*, 2015; Ahrlund-Richter *et al.*, 2009; Preti, 2005; Parson, 2006; and Dodson and Levine, 2015). However, several challenges arise when basic operations, such as product purification, are scaled-up (Soares *et al.*, 2014). As examples, Fluorescent Activated Cell Sorting and Magnetic Activated Cell Sorting (FACS and MACS, respectively) are well-established procedures for cell purification, but these techniques rely on expensive protein labels and have a limited throughput (ml/h) (Jan Krüger, 2002 and Cho *et al.*, 2010). Various microfluidic-based systems are emerging as label-free alternatives to sort cells at a higher throughput (ml/min), using inertial focusing (Di Carlo *et al.*, 2007; Wang *et al.*, 2013; Miller *et al.*, 2016), deterministic lateral displacement (Davis *et al.*, 2006 and Huang *et al.*, 2004),

[a)]Author to whom correspondence should be addressed: eg100@hw.ac.uk. Tel.: 01314514748.

pinch flow fractionation (Yamada *et al.*, 2004), or hydrodynamic filtration (Matsuda *et al.*, 2011) to mention a few. These approaches commonly consist of a micrometer size channel where cells' endogenous properties (i.e., size and/or deformability) are exploited for separation in a continuous manner. One of the remaining bottlenecks with such microsystems is their tendency to clog (Yoon *et al.*, 2016 and Dressaire and Sauret 2016) due to the channel cross-section being merely larger than a couple of cell diameters. One of the most commonly accepted solutions to prevent clogging issues is the use of additives such as poloxamers, dextran, or methylcellulose (Chisti, 2000).

Among these additives, Pluronic F-68 is a biocompatible amphiphilic and nonionic compound consisting of a central polyoxypropylene (POP) block, flanked on both sides by hydrophilic chains of polyoxyethylene (POE) (Alexandridis and Alan Hatton, 1995). This surface-active macromolecule (molecular weight, 8400) is used as an antifoam agent in stirred cell culture vessels and large scale bioreactors (Goldblum *et al.*, 1990; Karleta *et al.*, 2010; and Tharmalingam *et al.*, 2008) among numerous other applications [e.g., as antithrombotic (O'Keefe *et al.*, 1996) or anti-inflammatory (Harting *et al.*, 2008) agents, an artificial blood emulsifier (Schmolka, 1975), or a skin wound cleanser (Rodeheaver *et al.*, 1980)].

Pluronic F-68 and other poloxamers have been adopted as coating agents and additives in microfluidic systems engineered for cell analysis (McClain *et al.*, 2003), lysis (Hargis *et al.*, 2011), separation (Tan *et al.*, 2013), and detection (Brouzes *et al.*, 2009), in microconstrictions for assessing cell mechanical properties (Lange *et al.*, 2017) and digital microfluidics (Luk *et al.*, 2008). Poloxamers added to a flow buffer can coat glass (Tan *et al.*, 2004), silicon (Sundblom *et al.*, 2010), Polydimethylsiloxane (PDMS) (Wong and Ho, 2009), and Poly(methyl methacrylate) (PMMA) (Son *et al.*, 2014)—materials commonly used for microfluidic fabrication. This kind of treatment prevents clogging, reagent adsorption, protein fouling, and cell-cell interaction, reduces electro-osmotic flow, and can provide cell protection against a high degree of shear stress (Au *et al.*,2011). This repair and protective mechanism of Pluronic on cells is not fully understood yet; however, some literature evidence suggests the direct interaction with the cell membrane causing cell stiffening (Maskarinec *et al.*, 2002 and Wu *et al.*, 2004). As mentioned previously, mechanical cell properties are seen as a potential marker for label-free separation with applications in large-scale bioprocessing. However, the observation that Pluronic can stiffen cells suggests that the use of such additives could potentially impact the performance of mechanical based purification approaches.

In this work, we investigated the effect of Pluronic F-68 on cells commonly used in microfluidic studies: Jurkat cells, red blood cells (RBCs), and human embryonic kidney (HEK) cells. The aim was to quantify if the addition of Pluronic F-68 significantly influenced the cell mechanotype, which would have implications for mechanical phenotype based downstream cellular processing. For the first time, observed changes were quantified using real-time deformability cytometry (RT-DC) (Otto *et al.*, 2015) to assess the short-term impact of Pluronic F-68, in comparison to controls with and without serum, at high-throughput (thousands events/min).

II. MATERIALS AND METHODS

A. Real-time deformability cytometry

Cell mechanical properties were assessed using a Real-Time Deformability Cytometer (RT-DC) as described in previous works (Mietke *et al.*, 2015; Otto *et al.*, 2015; and Xavier *et al.*, 2016). Briefly, a PDMS channel consisting of three sections, two reservoir sections and one constriction channel (20 μm $\times$ 20 μm cross section), where cells undergo deformation and measurements, are undertaken (SFig. 1). Cells were pumped into the channel at two different flow rates of 0.04 (Jukrat and HEK) and 0.12 (red blood cells) μl/s, generating a shear stress (corresponding to approximately 1.2 and 4 kPa, respectively), resulting in cell deformation. The RT-DC system employs image processing algorithms which enable the measurement of the cell area and deformation. Deformation (D) is expressed as a deviation from a perfect circle

$$D = 1 - c, \tag{1}$$

where c is the circularity which is defined as

$$c = 2\sqrt{\pi A}/l, \tag{2}$$

with A being the projected cell area and l the cell perimeter. Deformation in the channel is independently measured from the initial cell shape and therefore any treatment-induced morphological changes to shape. Consequently, a differential deformation (DD) parameter has been introduced (Herbig *et al.*, 2018). DD includes morphological information acquired in the reservoir section of the RT-DC chip (where applied shear is negligible) by subtracting this value from the deformation measured in the channel. Subtraction is done by statistical representations of channel and reservoir measurements and using a bootstrapping approach (Golfier *et al.*, 2017 and Herbig *et al.*, 2018). RT-DC data were analysed using the ShapeOut 0.8.4 software (available at www.zellmechanic.com). Further analysis was performed using MatLab R2016b and GraphPad Prism 7. P-values were calculated using the linear mixed model.

B. Viability study

Jurkat cell viability was assessed using the Live/Dead Viability/Cytotoxicity kit for mammalian cells (Life Technologies Ltd.) as per the manufacturer's manual. The flow cytometric analysis was performed with excitation at 488 nm. Live cells stained with calcein emit green fluorescence (530/30 bandpass), while dead cells appear red (610/20 bandpass) due to staining with ethidium homodimer. Cells were analysed on a FACSCalibur machine (BD Bioscience) immediately after staining, and obtained raw data were analysed using FlowJo V10 CL software.

C. Cell culture and treatment

1. Sample preparation

a. Jurkat cells. Jurkat cells were cultured in Roswell Park Memorial Institute (RPMI) medium (ThermoFisher Scientific) supplemented with 10% (v/v) fetal bovine serum (FBS) (Gibco) in a humidified incubator at 37 °C in 5% CO_2. Cells from the same batch were collected and when at their exponential growth phase split into fresh cell culture flask to maintain researched conditions: a control incubated in medium with serum, a sample from complete medium supplemented with Pluronic F-68, cells incubated in PBS-/- (phosphate buffered saline without calcium and magnesium, Gibco, cat. 10010023), and PBS-/- containing Pluronic F-68 and incubated for desired times (1, 2, and 3 h) in a humidified incubator at 37 °C in 5% CO_2. The chosen time scale is motivated by an approximate time required to perform experiments using microfluidic systems, ensuring unaffected cell viability for unbiased results (SFig. 2). Prior to RT-DC measurements, cells were collected by centrifugation at $300 \times g$ for 5 min and re-suspended in 0.5% (w/v) solution of methylcellulose at 1×10^6 cells/ml. To assess the effect of the Pluronic F-68 concentration, the concentration was adjusted to 0.1%, 0.5%, and 1% (w/v) and quantified after 3 h incubation. At each time point, cells from both tubes (control and treated samples) were collected by centrifugation and re-suspended in 0.5% methylcellulose and immediately taken for measurements in the RT-DC. All obtained data result from three independent replicates, from cells of the same cell line coming from different batches.

b. Red blood cells. Packed purified red blood cells (RBCs) from healthy donors stored in a serum-free buffer were purchased from Cambridge Bioscience Ltd. Cells were stored at 4 °C, and cells from three batches were used for experimental work within a week of collection. Cells for experiments were counted on a haemocytometer, and the cell density was adjusted to 10×10^6 cells/ml by addition of an adequate PBS-/- volume (experimental control) or PBS-/- supplemented with Pluronic F-68 to a 1% (w/v) final concentration. Prepared cells were

incubated at 4 °C prior to measurements on RT-DC, then collected by centrifugation at 500 × g for 5 min, and re-suspended in 0.5% methylcellulose.

c. HEK cells. HEK cells were cultured in basal Dulbecco's Modified Eagle Medium (DMEM) (ThermoFisher Scientific) supplemented with 10% (v/v) FBS (Gibco) and 1% (v/v) GlutaMAX™ (ThermoFisher Scientific) in a humidified incubator at 37 °C in 5% CO_2. Cells from the same batch were collected for RT-DC measurements by harvesting them into the suspension using TrypLE™ (ThermoFisher Scientific). Prior to the TrypLE treatment, cells were washed twice with PBS-/-, and an appropriate volume (5 ml for a 75 cm^2 flask) of TrypLE was added. Cells were incubated in a humidified incubator at 37 °C in 5% CO_2 for 5 min. After the monolayer dissociation, complete medium containing serum was added to inactivate the TrypLE and wash cells off the surface of the flask. Next, cells were transferred into a 15 ml centrifuge tube, and they were collected by centrifugation at 300 × g for 5 min, the supernatant was discarded, and cells were re-suspended in 0.5% solution of methylcellulose at 1×10^6 cells/ml. A control containing serum was collected straight from the cell culture flask. The remaining two samples were cultured for 1, 2, and 3 h in either (PBS-/-) (serum-free experiment) or PBS-/- supplemented with 1% (w/v) cell culture grade Pluronic F-68 (ThermoFisher Scientific) (treated sample), incubated for a desired time in a humidified incubator at 37 °C in 5% CO_2, and harvested prior to measurements as described above. All obtained data results from three independent replicates, from cells of the same cell line coming from different batches.

HEK cells were also examined for cytoskeletal re-arrangements in their adherent and suspended states by examining F-actin. Cells (adherent and harvested in suspension HEK in serum control, HEK incubated for 3 h in PBS, and PBS supplemented with 1% Pluronic F-68) were stained for 30 min at room temperature against F-actin with Actin Creen 488 Ready Probes reagents (Life Technologies, cat. R37110). 10 min before the end of the incubation time, Hoechst 33342 (Sigma Aldrich, cat. 14533) was added to a final 10 ng/ml concentration to visualise the cell nucleus. To avoid additional cytoskeletal re-arrangements due to cell preparation for microscopy, cells after treatment were fixed in 4% paraformaldehyde (PFA) (ThermoFisher Scientific, cat. 28906). Acquisition was performed on a Leica SP5 SMD (Single Molecule Detection) confocal laser-scanning microscope using a 63 × 1.4 NA HCX PL Apo oil immersion objective lens. Actin Creen 488 was excited using a tunable white light laser operating at 488 nm and a pulse rate of 80 MHz. Hoechtst 33342 was excited with a pulsed 405 nm laser at a pulse rate of 40 MHz. Emission was detected with a photon multiplier tube (PMT).

III. RESULTS

A. Effect of Pluronic on Jurkat cell size and deformability

1. Time dependency

To understand the short-term effect of the Pluronic F-68 additive on the cell mechanotype, we measured the size and deformability of Jurkat cells cultured either in cell culture medium containing serum or phosphate-buffered saline (PBS-/-), and we compared them against cells whose medium was supplemented with 1% Pluronic F-68. The choice of a serum-free experiment is motivated by our experience with microfluidic systems. Most tissue culture systems contain serum, which easily clogs microfluidic chips (due to the high protein content), and therefore, replacing the cell culture medium with PBS-/- for the time of the experiments is a common practice (McGrath *et al.*, 2014; Lange *et al.*, 2017; and Abd Rahman *et al.*, 2017). The RT-DC measurements were taken each hour for 3 h. The chosen time-scale was motivated by an average longevity of experiments in microfluidic systems used in our laboratory.

Figures 1(a) and 1(b) show time-dependent changes in cell deformability. The effect of Pluronic F-68 was normalised to the untreated control. For both conditions, addition of Pluronic F-68 causes significant changes after 3 h of addition. The alteration of deformability, expressed here as differential deformation (DD) (please see materials and methods for details) of cells cultured in serum [Fig. 1(a)], progresses slowly but gradually for the first 2 h, causing initially

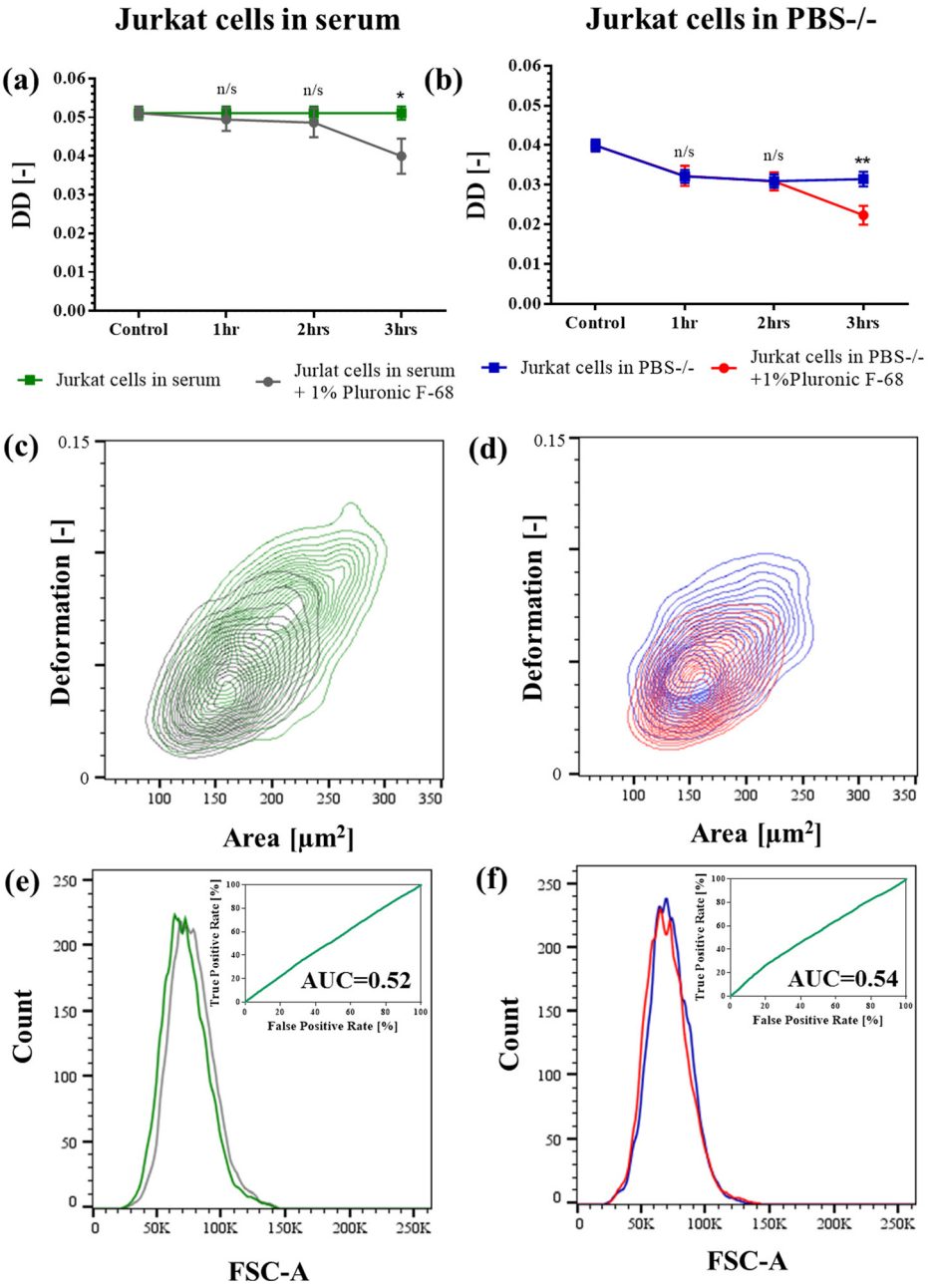

FIG. 1. Effect of Pluronic F-68 on cells of Jurkat cell line mechanical properties was quantified using real-time deformability cytometry (RT-DC) and flow cytometry. Cells from four conditions: Jurkat cells in serum (green)—cells extracted directly from tissue culture containing serum; Jurkat cells in serum +1% (w/v) Pluronic F-68 (gray)—cells cultured in medium containing serum supplemented with 1% Pluronic F-68; Jurkat cells in PBS-/- (blue)—cells incubated in PBS-/- without serum; and Jurkat cells in PBS-/- +1% Pluronic F-68 (red)—cells incubated in PBS-/- supplemented with 1% Pluronic F-68, without serum, were examined. Deformation was measured every hour for 3 h. (a) and (b) Time-dependent response graphs show mean differential deformation (DD) values of three experimental replicates. Error bars correspond to the standard error of the mean (SEM). P-values were calculated using the linear mixed model (*p-value < 0.01, **p-value < 0.001, and n/s = no significant). (c) and (d) Exemplary contour plots show outlines of assessed populations (more than 4000 events per population) for deformation versus size (expressed as the projected cell area in μm^2) recorded in the measurement channel section of the RT-DC chip. All samples were examined at a flow rate of 0.04 μl/s in a 20 $\times$ 20 μm^2 cross sectional RT-DC channel after 3 h of incubation. (e) and (f) Cell size was assessed using the forward light scatter parameter (FSC-A) measured using a flow cytometer for 10 000 cells. Receiver Operating Characteristic (ROC) curves were plotted for size expressed as FSC-A. The true positive rate is defined as the number of control cells measured for a certain size cutoff point and divided by the total number of control cells. The false positive rate is the corresponding number of Pluronic F-68-treated cells divided by the total number of treated cells for the same cutoff. The area under the curve (AUC) was calculated to quantify the size overlap between control and treated cells after 3 h.

slight (>5%), almost negligible (p-value, no significant), stiffening. Incubating cells for 3 h in the presence of Pluronic F-68 causes significant (p-value <0.01) decreases in cell deformability (∼23%). Specifically, it drops within 3 h from DD = 0.051 ± 0.0017 to DD = 0.039 ± 0.0045 (DD is expressed as the mean of three experimental replicates ± standard error of the mean, SEM).

Interestingly, when the medium containing serum is replaced with PBS-/- [control from Fig. 1(b)], cell deformability drops by ∼22% from the original DD = 0.051 ± 0.0017 to DD = 0.040 ± 0.0015 within less than 15 min of medium replacement, and it equilibrates within an hour at DD = 0.032 ± 0.0016. During the first 2 h, the Pluronic F-68-treated sample and PBS-/- control are indistinguishable. After 3 h of incubation, the Pluronic F-68-treated sample diverges and becomes stiffer (DD = 0.022 ± 0.0023) by ∼29%.

The RT-DC technique is based on image analysis allowing for the size measurement, which is expressed as a projected cell area reported in μm^2, as shown in the contour plots [Figs. 1(c) and 1(d)]. Typically, the cell size is obtained from images acquired in the reservoir section (SFigs. 1 and 3) where the degree of shear is negligible, ensuring the best cell alignment. Although accurate, the technique can at times be sensitive to the changes in focus setting. Hence, rather than reporting the projected cell area, we used flow cytometry to quantify forward light scatter (FSC-A)—a measurement of the amount of a laser beam that passes around the cell—providing a relative cell size. Figures 1(e) and 1(f) show the acquired values of FSC-A for all conditions. To quantify the degree of size overlap, receiver operating curves (ROC) were generated, and the corresponding area under the curve (AUC) was calculated. Supplementing the medium with Pluronic F-68 has a negligible effect on cell size, and it remains unchanged for both cells in serum (AUC = 0.52) and cells in PBS-/- (AUC = 0.54).

2. Concentration dependency

Recommended poloxamer additive concentrations depend on the purpose and intended application. Proposed working concentrations for cell culture vary between 0.1% and 1% w/v (Gigout *et al.*, 2008; Guo *et al.*, 2014; and Tharmalingam *et al.*, 2008). Here, we examined the effect of different Pluronic F-68 concentrations (0.1, 0.5, and 1% w/v) on Jurkat cells, incubated for 3 h in the supplemented medium with and without serum and compared to untreated controls.

Figure 2 shows the effect of different Pluronic F-68 concentrations on Jurkat cells in serum exerted in terms of cell deformability. Lower concentrations (0.1% and 0.5%) do not trigger changes in cell deformability within the first 3 h of exposure. The cell size (expressed as FSC-A measured by flow cytometry) remains unaffected as reported in Fig. 2(b) (AUC = 0.53 for 1%, AUC = 0.50 for 0.5%, and AUC = 0.54 for 0.1% Pluronic F-68).

Jurkat cells in PBS-/- [Fig. 2(c)] are slightly more sensitive to the presence of Pluronic F-68 since small (∼ 6%) but consistent changes (standard error of the mean SEM = 0.0007 for three replicates of the experiment, p-value < 0.01) are observed after 3 h of exposure to 0.5% Pluronic F-68. Similar to the previous samples, the cell size remains unaffected for all conditions [Fig. 2(d)].

B. Effect of Pluronic F-68 on RBC size and deformability

In previous works, the effect of Pluronic F-68 on red blood cells (RBCs) was examined for diseased erythrocytes in sickle anaemia, where it was discovered that Pluronic F-68 minimises cell-cell adherence and blood viscosity (Smith *et al.*, 1987 and Sandor *et al.*, 2015). Here, we focused on the impact of Pluronic on mechanical properties, and we compared the deformation of packed RBCs stored in a serum-free buffer and RBCs treated with 1% Pluronic F-68 over the course of 3 h. Figures 3(a) and 3(b) demonstrate that the stiffening effect observed for Jurkat cells, when incubated for a short time (up to 3 h) in poloxamer additives, is also shown by RBCs, however, to a smaller degree. A decrease in RBC deformation from its original value DD = 0.164 ± 0.008 is visible after 2 h of incubation (DD = 0.148 ± 0.006). Initially, cell deformation drops by ∼10% (p-value < 0.01) to reach ∼− 16% (DD = 0.135 ± 0.008,

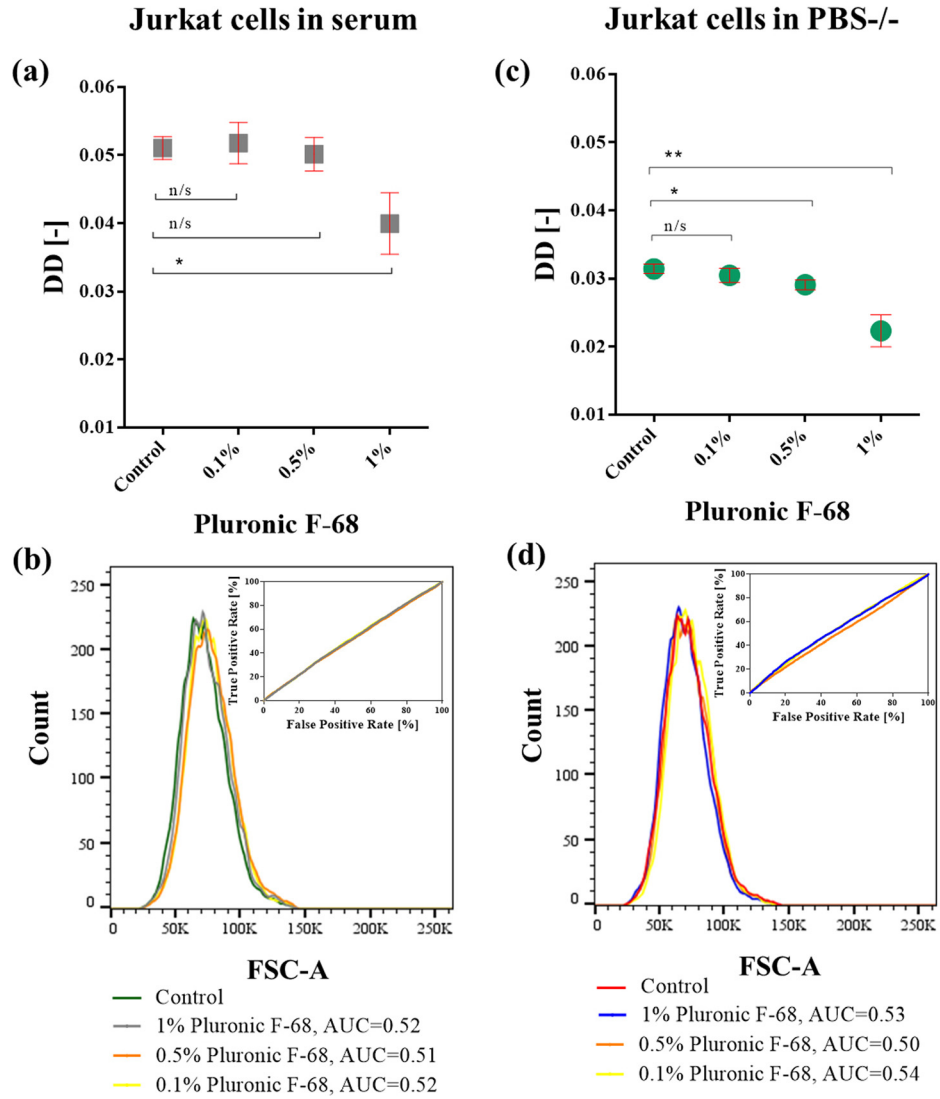

FIG. 2. Cells of the Jurkat cell line were used to examine concentration-dependent deformability and size alteration caused by the Pluronic F-68 additive. Cells were incubated for 3 h in medium containing serum and PBS-/- supplemented with 0.1% (yellow), 0.5% (orange), and 1% (grey) Pluronic F-68. (a) and (c) Concentration-dependent graphs show that Jurka cells response to the increasing concentration of Pluronic F-68 in comparison to untreated control. The data points represent the mean differential deformation (DD) values of Jurkat cells treated with Pluronic F-68 measured on three separate occasions. The bar graphs represent the standard error of the mean (SEM), and the significance of results was calculated using the linear mixed model (* p-value < 0.01, ** p-value < 0.001, and n/s = no significant). (b) and (d) To assess if treatment with Pluronic F-68 causes changes in size, cells were characterised by flow cytometry for the forward light scatter (FSC-A) for 100 00 cells from each condition. Receiver Operating Characteristic (ROC) curves were plotted for size expressed as FSC-A. The true positive rate is defined as the number of control cells measured for a certain size cutoff point and divided by the total number of control cells (green). The false positive rate is the corresponding number of Pluronic F-68-treated cells divided by the total number of treated cells for the same cutoff. The area under the curve (AUC) was calculated to quantify the size overlap between control and treated cells. Data for all samples were collected at a flow rate of 0.04 μl/s in a 20×20 μm^2 cross sectional RT-DC channel.

p-value < 0.01) after 3 h of exposure to Pluronic F-68. RBCs are not spherical, while in the suspension, they are biconcave discs, and when exposed to shear in laminar flow, they streamline and assemble the tear-like shape as shown in Fig. 3(c). To assess if exposure to Pluronic F-68 causes changes in the size, RBCs from both conditions at the 3 h time-point were assessed by flow cytometry for the FSC-A parameter [Fig. 3(d)]. A ROC curve with AUC = 0.52 was generated to confirm that the cell size is unaffected by short-term exposure to Pluronic F-68.

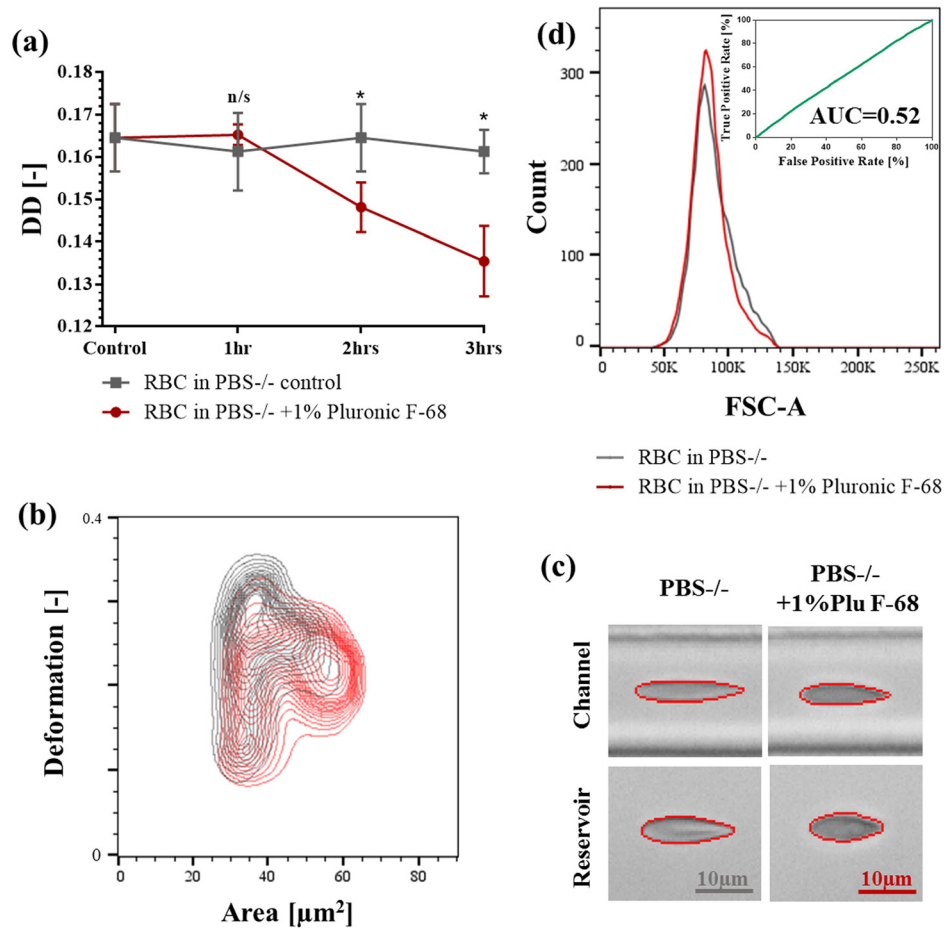

FIG. 3. Deformability and size of isolated packed red blood cells (RBCs) treated with 1% Pluronic F-68 (red) were compared to untreated control (grey). Both samples were examined at a flow rate of 0.12 μl/min in a 20×20 μm^2 cross-sectional RT-DC channel. (a) Time-dependent alteration in deformability as a response to 1% Pluronic F-68 is presented as mean differential deformation (DD) values measured on three separate occasions. The error bars are the standard error of the mean. P-values were calculated using the standardized mixed model (*p-value < 0.01 and n/s = no significant). (b) Contour plots (for more than 2000 cells from each population) were drawn, presenting cell deformability vs projected cell area (μm^2). (c) Representative images of cells extracted from the channel and reservoir section of the RT-DC chip for cells incubated for 3 h. (d) To assess if treatment with Pluronic F-68 causes changes in size, cells (10 000 events for each condition) were characterised by flow cytometry for the forward light scatter (FSC-A). Receiver Operating Characteristic (ROC) curves were plotted for size expressed as FSC-A. The true positive rate is defined as the number of control cells measured for a certain size cutoff point and divided by the total number of control cells (green). The false positive rate is the corresponding number of Pluronic F-68-treated cells divided by the total number of treated cells for the same cutoff. The area under the curve (AUC) was calculated to quantify the size overlap between control and treated cells.

C. Effect of Pluronic F-68 on adherent HEK cells

Human embryonic kidney (HEK) cells are adherent cells commonly used in cell biology (Stepanenko and Dmitrenko, 2015). Due to the wide-spread application of HEK cells, we used this cell line to research if there is a short-term (1–3 h exposure) effect of Pluronic F-68 exerted on adherent cells, using the same methodology as presented above. Deformability of cells cultured in the medium with serum, incubated in PBS-/- and PBS-/- supplemented with 1% Pluronic F-68, was examined [Figs. 4(a) and 4(b)]. Prior to the measurement, cells were harvested into the suspension by enzymatic treatment with TrypLE [Fig. 4(c)]. The enzymatic harvest protocol requires serum removal to prevent enzyme inhibition. The serum is removed by replacing the cell culture medium with PBS-/- and washing with PBS-/- in order to remove traces of the protein-rich serum. Figure 4(a) shows changes in deformation measured by RT-

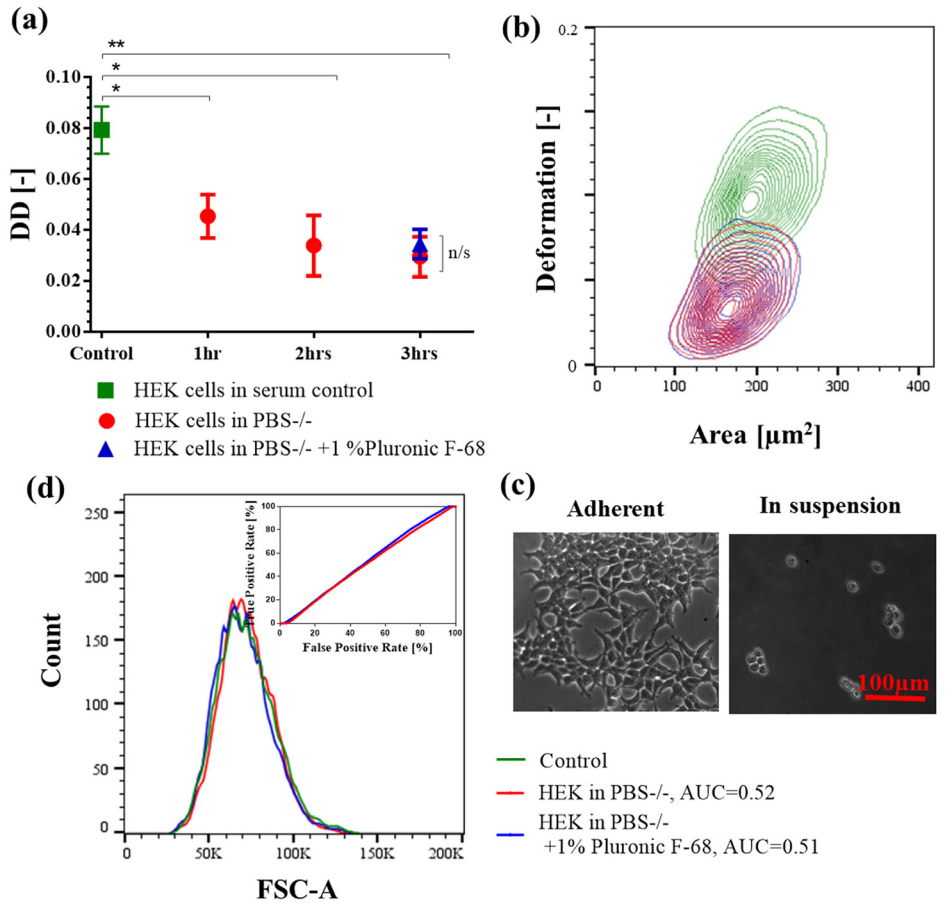

FIG. 4. Effect of Pluronic F-68 on adherent HEK cell deformability was quantified using real-time deformability cytometry. Cells from three conditions: HEK cells in serum (green)—cells harvested directly from tissue culture containing serum; HEK cells in PBS-/- (red)—cells incubated in PBS-/- without serum for 1, 2, and 3 h; and HEK cells in PBS-/- +1% Pluronic F-68 (blue)—cells incubated in PBS-/- supplemented with 1% Pluronic F-68, without serum, were examined in a 20×20 μm^2 cross-sectional RT-DC channel at a flow rate of 0.04 μl/s. (a) Time-dependent response graphs show the mean differential deformation (DD) values of three experimental replicates. Error bars correspond to the standard error of the mean (SEM). P-values were calculated using the linear mixed model (*p-value $<$ 0.01, ** p-value $<$ 0.001, and n/s = no significant). (b) Exemplary contour plots show outlines of assessed populations for deformation vs size (expressed as the projected cell area in μm^2) recorded in the measurement channel section of the RT-DC chip for more than 4000 cells. (c) Prior to the measurement, cells were harvested into the suspension using enzymatic treatment. Representative images obtained at $\times$20 magnification show the morphology of adherent cells and cells in the suspension. (d) Cell size was assessed by flow cytometry for the forward light scatter (FSC-A) for 10 000 cells from each condition. Receiver Operating Characteristic (ROC) curves were plotted for size expressed as FSC-A. The true positive rate is defined as the number of control cells measured for a certain size cutoff point and divided by the total number of control cells (green). The false positive rate is the corresponding number of treated cells (either in PBS-/- or PBS-/- +1% Pluronic F-68, respectively) divided by the total number of treated cells for the same cutoff. The area under the curve (AUC) was calculated to quantify the size overlap between control and treated cells.

DC for HEK cells cultured in PBS-/- (red) and PBS-/- supplemented with 1% Pluronic F-68 (blue) for 3 h and compared control cells (green) cultured in the whole cell culture medium. There was no significant (p-value n/s) change observed between PBS-/- cells (DD = 0.029 $\pm$ 0.0078) and PBS-/- + 1% Pluronic F-68 (DD = 0.034 $\pm$ 0.0058). The most dramatic change ($\sim -63\%$ after 3 h, p-value $<$0.001) was triggered by replacing the whole medium (DD = 0.079 $\pm$ 0.0093) with PBS-/-. To assess if replacing the cell culture medium with PBS-/- and PBS-/- supplemented with 1% Pluronic F-68 triggers any changes in size, cells were assessed by flow cytometry for the FSC-A parameter [Fig. 4(d)]. Despite the dramatic change in cell deformation caused by replacing the whole medium with PBS/-/, there is no size alteration (AUC = 0.52). Similarly, supplementing PBS-/- buffer with 1% Pluronic F-68 does not contribute to cell size alteration (AUC = 0.51).

IV. DISCUSSION AND CONCLUSION

In this study, it was demonstrated that Pluronic F-68 alters cell mechanical properties, causing cell stiffening with no impact on cell size. The short-time (1–3 h) effect was examined for cells of the Jurkat (suspension) cell line, red blood cells, and adherent HEK cells. It was established that cell deformability undergoes significant alteration within the first hours of exposure to Pluronic F-68, even at concentrations as low as 0.5% w/v for cells in the suspension without serum. Adherent HEK cells do not show the stiffening trend as observed for Jurkat cells and RBCs. We speculate that the result could be explained with the cell preparation protocol since prior to RT-DC measurements (similar to other common microfluidic applications), HEK cells have to be harvested into the suspension. We believe that the harvest exerts more dramatic effects than the Pluronic treatment itself. By imaging HEK cells, we observed that cell detachment is followed by changes in cytoskeleton (SFig. 4), known to substantially contribute to cell mechanical properties (Walther *et al.*, 2016). More specifically, when cells adhere to a surface, the F-actin (in green in SFig. 4) spreads, creating angular shapes surrounding the cell nucleus (in blue in SFig. 4). When cells are harvested into the suspension, F-actin rearranges to maintain a spherical shape, with the characteristic sharp-corners being replaced with some irregular round local accumulations of F-actin and smooth appearance.

The cell mechanical response to treatment with Pluronic F-68 is relatively small, and due to Pluronic biocompatible nature, they are physiologically negligible (with no effect on cell size and viability). However, it must be considered that cell deformability can be significantly affected by the poloxamer additive and serum removal from the experimental system. It has been shown that Pluronic F-68 decreases plasma membrane fluidity (Ramirez and Mutharasan, 1990), probably due to its surfactant properties, enabling Pluronic to integrate into the lipid bilayer of the cell (Maskarinec *et al.*, 2002). Although the exact mechanism underpinning cell stiffening after exposure to Pluronic F-68 is not known yet, Gigout *et al.* tracked Pluronic F-68 uptake within Jurkat cells, discovering that fluorescently tagged Pluronic F-68 is continually transferred into the cell, enclosed in endosomes, and transported alongside the endocytotic pathway. Based on these results, they suggested that the stiffening effect could be explained partially by the alteration of the cell membrane and cytoplasm properties, as a consequence of the high Pluronic content accumulated in intracellular vesicles localised across the cytoplasm and just beneath the plasma membrane.

Cell deformability is gaining recognition as a novel cell state marker. Reduced cell deformability is commonly associated with a pathological phenotype, e.g., in malaria (Hosseini and Feng, 2012 and Toepfner *et al.*, 2018), sickle-cell disease (Xu *et al.*, 2016), and thalassemia (Athanasiou *et al.*, 1991). Additionally, deformability is seen as a valuable label-free marker associated with various cell activities, such as cell cycle regulation (Tsai *et al.*, 1996), differentiation (Lin *et al.*, 2017), metastasis (Ochalek *et al.*, 1988), and leukocyte activation (Khismatullin, 2009). Many available technologies for deformability analysis [Atomic Force Microscopy (Jalili and Laxminarayana 2004), microconstrictions (Lange *et al.*, 2015), optical stretchers (Ekpenyong *et al.*, 2012), micropipette aspiration (Kee and Robinson, 2013), and magnetic bead twisting (Wang *et al.*, 1993)] require prolonged operational time to gain a reasonable number of measurements. Our findings highlight the importance of seeking high-throughput technologies and careful consideration of experimental conditions to measure deformability changes and analyse the mechanical phenotype.

SUPPLEMENTARY MATERIAL

See supplementary material for the RT-DC setup schematic and flow cytometric viability assay results.

ACKNOWLEDGMENTS

We wish to thank the Industrial Biotechnology Innovation Centre (IBioIC) for providing resources for this research. M.J. would like to thank the Engineering and Physical Sciences Research Council (EPSRC) for her personal Research Fellowship. O.O. gratefully acknowledges

the support from the Federal Ministry of Education and Research of Germany (ZIK Grant under Agreement No. 03Z22CN11).

We would like to acknowledge ZELLMECHANIK DRESDEN for providing us access to the Real-Time Deformability Cytometer (RT-DC) and especially thank Christoph Herold for his technical support and assistance.

O.O. is the co-founder of ZELLMECHANIK DRESDEN distributing real-time deformability cytometry.

We gratefully acknowledge the support offered by the MRC-funded Edinburgh Super-Resolution Imaging Consortium for both their expertise and infrastructure.

Abd Rahman, N., Ibrahim, F., and Yafouz, B., "Dielectrophoresis for biomedical sciences applications: A review," Sensors (Basel) **17**(3), 449 (2017).

Ahrlund-Richter, L., De Luca, M., Marshak, D. R., Munsie, M., Veiga, A., and Rao, M., "Isolation and production of cells suitable for human therapy: Challenges ahead," Cell Stem Cell **4**(1), 20–26 (2009).

Alexandridis, P. and Alan Hatton, T., "Poly(ethylene oxide)·poly(propylene oxide)·poly(ethylene oxide) block copolymer surfactants in aqueous solutions and at interfaces: Thermodynamics, structure, dynamics, and modeling," Colloids Surf. A **96**(1), 1–46 (1995).

Athanasiou, G., Zoubos, N., and Missirlis, Y., "Erythrocyte membrane deformability in patients with thalassemia syndromes," Nouv. Rev. Fr. Hematol. **33**(1), 15–20 (1991).

Au, S. H., Kumar, P., and Wheeler, A. R., "A new angle on pluronic additives: Advancing droplets and understanding in digital microfluidics," Langmuir **27**(13), 8586–8594 (2011).

Brouzes, E., Martina, M., Neal, S., Dave, M., Mariusz, T., Brian Hutchison, J., Rothberg, J. M., Link, D. R., Norbert, P., and Samuels, M. L., "Droplet microfluidic technology for single-cell high-throughput screening," Proc. Natl. Acad. Sci. U. S. A. **106**(34), 14195–14200 (2009).

Chisti, Y., "Animal-cell damage in sparged bioreactors," Trends Biotechnol. **18**(10), 420–432 (2000).

Cho, S. H., Chen, C. H., Tsai, F. S., Godin, J. M., and Lo, Y. H., "Human mammalian cell sorting using a highly integrated micro-fabricated fluorescence-activated cell sorter (microFACS)," Lab Chip **10**(12), 1567–1573 (2010).

Davis, J. A., Inglis, D. W., Morton, K. J., Lawrence, D. A., Huang, L. R., Chou, S. Y., Sturm, J. C., and Austin, R. H., "Deterministic hydrodynamics: Taking blood apart," Proc. Natl. Acad. Sci. U. S. A. **103**(40), 14779–14784 (2006).

Di Carlo, D., Irimia, D., Tompkins, R. G., and Toner, M., "Continuous inertial focusing, ordering, and separation of particles in microchannels," Proc. Natl. Acad. Sci. U. S. A. **104**(48), 18892–18897 (2007).

Dodson, B. P. and Levine, A. D., "Challenges in the translation and commercialization of cell therapies," BMC Biotechnol. **15**(1), 70 (2015).

Dressaire, E. and Sauret, A., "Clogging of microfluidic systems," Soft Matter **13**(1), 37–48 (2016).

Ekpenyong, A. E., Whyte, G., Chalut, K., Pagliara, S., Lautenschläger, F., Fiddler, C., Paschke, S., Keyser, U. F., Chilvers, E. R., and Guck, J., "Viscoelastic properties of differentiating blood cells are fate- and function-dependent," PLoS One **7**(9), e45237 (2012).

Gigout, A., Buschmann, M. D., and Jolicoeur, M., "The fate of Pluronic F-68 in chondrocytes and CHO cells," Biotechnol. Bioeng. **100**(5), 975–987 (2008).

Goldblum, S., Bae, Y. K., Hink, W. F., and Chalmers, J., "Protective effect of methylcellulose and other polymers on insect cells subjected to laminar shear stress," Biotechnol. Prog. **6**(5), 383–390 (1990).

Golfier, S., Rosendahl, P., Mietke, A., Herbig, M., Guck, J., and Otto, O., "High-throughput cell mechanical phenotyping for label-free titration assays of cytoskeletal modifications," Cytoskeleton (Hoboken, NJ) **74**(8), 283–296 (2017).

Guo, Q., Duffy, S. P., Matthews, K., Santoso, A. T., Scott, M. D., and Ma, H., "Microfluidic analysis of red blood cell deformability," J. Biomech. **47**(8), 1767–1776 (2014).

Hargis, A. D., Alarie, J. P., and Ramsey, J. M., "Characterization of cell lysis events on a microfluidic device for high-throughput single cell analysis," Electrophoresis **32**(22), 3172–3179 (2011).

Harting, M. T., Jimenez, F., Kozar, R. A., Moore, F. A., Mercer, D. W., Hunter, R. L., Cox, C. S., and Gonzalez, E. A., "Effects of Poloxamer 188 on human PMN cells," Surgery **144**(2), 198–203 (2008).

Heathman, T. R., Nienow, A. W., McCall, M. J., Coopman, K., Kara, B., and Hewitt, C. J., "The translation of cell-based therapies: Clinical landscape and manufacturing challenges," Regener. Med. **10**(1), 49–64 (2015).

Herbig, M., Krater, M., Plak, K., Muller, P., Guck, J., and Otto, O., "Real-time deformability cytometry: Label-free functional characterization of cells," Methods Mol. Biol. **1678**, 347–369 (2018).

Huang, L. R., Cox, E. C., Austin, R. H., and Sturm, J. C., "Continuous particle separation through deterministic lateral displacement," Science **304**(5673), 987–990 (2004).

Jalili, N. and Laxminarayana, K., "A review of atomic force microscopy imaging systems: Application to molecular metrology and biological sciences," Mechatronics **14**(8), 907–945 (2004).

Karleta, V., Andrlik, I., Braunmuller, S., Franke, T., Wirth, M., and Gabor, F., "Poloxamer 188 supplemented culture medium increases the vitality of Caco-2 cells after subcultivation and freeze/thaw cycles," Altex **27**(3), 191–197 (2010).

Kee, Y. S. and Robinson, D. N., "Micropipette aspiration for studying cellular mechanosensory responses and mechanics," Methods Mol. Biol. **983**, 367–382 (2013).

Khismatullin, D. B., "The cytoskeleton and deformability of white blood cells," in *Current Topics in Membranes* (Academic Press, 2009), Chap. 3, pp. 47–111.

Krüger, J., Singh, K., O'Neill, A., Jackson, C., Morrison, A., and O'Brien, P., "Development of a microfluidic device for fluorescence activated cell sorting," J. Micromech. Microeng. **12**(4), 486–494 (2002).

Lange, J. R., Steinwachs, J., Kolb, T., Lautscham, L. A., Harder, I., Whyte, G., and Fabry, B., "Microconstriction arrays for high-throughput quantitative measurements of cell mechanical properties," Biophys. J. **109**(1), 26–34 (2015).

Lange, J. R., Metzner, C., Richter, S., Schneider, W., Spermann, M., Kolb, T., Whyte, G., and Fabry, B., "Unbiased high-precision cell mechanical measurements with microconstrictions," Biophys. J. **112**(7), 1472–1480 (2017).
Lin, J., Kim, D., Tse, H. T., Tseng, P., Peng, L., Dhar, M., Karumbayaram, S., and Di Carlo, D., "High-throughput physical phenotyping of cell differentiation," Microsyst. Nanoeng. **3**, 17013 (2017).
Luk, V. N., GCh, M., and Wheeler, A. R., "Pluronic additives: A solution to sticky problems in digital microfluidics," Langmuir **24**(12), 6382–6389 (2008).
Majid Hosseini, S. and Feng, J. J., "How malaria parasites reduce the deformability of infected red blood cells," Biophys. J. **103**(1), 1–10 (2012).
Maskarinec, S. A., Hannig, J., Lee, R. C., and Lee, K. Y., "Direct observation of poloxamer 188 insertion into lipid monolayers," Biophys. J. **82**(3), 1453–1459 (2002).
Mason, C., Brindley, D. A., Culme-Seymour, E. J., and Davie, N. L., "Cell therapy industry: Billion dollar global business with unlimited potential," Regener. Med. **6**, 265–272 (2011).
Matsuda, M., Yamada, M., and Seki, M., "Blood cell classification utilizing hydrodynamic filtration," Electron. Commun. Jpn. **94**(1), 1–6 (2011).
McClain, M. A., Culbertson, C. T., Jacobson, S. C., Allbritton, N. L., Sims, C. E., and Ramsey, J. M., "Microfluidic devices for the high-throughput chemical analysis of cells," Anal. Chem. **75**(21), 5646–5655 (2003).
McGrath, J., Jimenez, M., and Bridle, H., "Deterministic lateral displacement for particle separation: A review," Lab Chip **14**(21), 4139–4158 (2014).
Mietke, A., Otto, O., Girardo, S., Rosendahl, P., Taubenberger, A., Golfier, S., Ulbricht, E., Aland, S., Guck, J., and Fischer-Friedrich, E., "Extracting cell stiffness from real-time deformability cytometry: Theory and experiment," Biophys. J. **109**(10), 2023–2036 (2015).
Miller, B., Jimenez, M., and Bridle, H., "Cascading and parallelising curvilinear inertial focusing systems for high volume, wide size distribution, separation and concentration of particles," Sci. Rep. **6**, 36386 (2016).
Ochalek, T., Nordt Fj Fau, K., Fau-Burger, M. M. T. K., and Burger, M. M., "Correlation between cell deformability and metastatic potential in B16-F1 melanoma cell variants," Cancer Res. **48**, 5124–5128 (1988).
O'Keefe, J. H., Grines, C. L., DeWood, M. A., Schaer, G. L., Browne, K., Magorien, R. D., Kalbfleisch, J. M., Fletcher, W. O., Jr., Bateman, T. M., and Gibbons, R. J., "Poloxamer-188 as an adjunct to primary percutaneous transluminal coronary angioplasty for acute myocardial infarction," Am. J. Cardiol. **78**(7), 747–750 (1996).
Otto, O., Rosendahl, P., Mietke, A., Golfier, S., Herold, C., Klaue, D., Girardo, S., Pagliara, S., Ekpenyong, A., Jacobi, A., Wobus, M., Topfner, N., Keyser, U. F., Mansfeld, J., Fischer-Friedrich, E., and Guck, J., "Real-time deformability cytometry: On-the-fly cell mechanical phenotyping," Nat. Methods **12**(3), 199–202 (2015).
Parson, A., "The long journey from stem cells to medical product," Cell **125**(1), 9–11 (2006).
Preti, R. A., "Bringing safe and effective cell therapies to the bedside," Nat. Biotechnol. **23**, 801–804 (2005).
Ramirez, O. T. and Mutharasan, R., "The role of the plasma membrane fluidity on the shear sensitivity of hybridomas grown under hydrodynamic stress," Biotechnol. Bioeng. **36**(9), 911–920 (1990).
Rao, M. S., "Funding translational work in cell-based therapy," Cell Stem Cell **9**(1), 7–10 (2011).
Rodeheaver, G. T., Kurtz, L., Kircher, B. J., and Edlich, R. F., "Pluronic F-68: A promising new skin wound cleanser," Ann. Emerg. Med. **9**(11), 572–576 (1980).
Sandor, B., Marin, M., Lapoumeroulie, C., Rabai, M., Lefevre, S., Lemonne, N., Nemer, W. E., Francais, O., Pioufle, B. L., Aronovicz, Y. C., Connes, P., and Kim, C. L. V., "Effects of Poloxamer 188 on red blood cells membrane properties in sickle cell disease," Blood **126**(23), 2174 (2015).
Schmolka, I. R., "Artificial blood emulsifiers," Fed. Proc. **34**(6), 1449–1453 (1975).
Smith, C. M., 2nd, Hebbel, R. P., Tukey, D. P., Clawson, C. C., White, J. G., and Vercellotti, G. M., "Pluronic F-68 reduces the endothelial adherence and improves the rheology of liganded sickle erythrocytes," Blood **69**(6), 1631–1636 (1987).
Soares, F. A. C., Chandra, A., Thomas, R. J., Pedersen, R. A., Vallier, L., and Williams, D. J., "Investigating the feasibility of scale up and automation of human induced pluripotent stem cells cultured in aggregates in feeder free conditions," J. Biotechnol. **173**(100), 53–58 (2014).
Son, H. Y., Lee, D. J., Lee, J. B., Park, C. H., Seo, M., Jang, J., Kim, S. J., Yoon, M. S., and Nam, Y. S., "In situ functionalization of highly porous polymer microspheres with silver nanoparticles via bio-inspired chemistry," RSC Adv. **4**(98), 55604–55609 (2014)..
Stepanenko, A. A. and Dmitrenko, V. V., "HEK293 in cell biology and cancer research: Phenotype, karyotype, tumorigenicity, and stress-induced genome-phenotype evolution," Gene **569**(2), 182–190 (2015).
Sundblom, A., Palmqvist, A. E. C., and Holmberg, K., "Study of the pluronic−silica interaction in synthesis of mesoporous silica under mild acidic conditions," Langmuir **26**(3), 1983–1990 (2010).
Tan, J. L., Liu, W., Nelson, C. M., Raghavan, S., and Chen, C. S., "Simple approach to micropattern cells on common culture substrates by tuning substrate wettability," Tissue Eng. **10**(5-6), 865–872 (2004).
Tan, S. J., Kee, M. Z., Mathuru, A. S., Burkholder, W. F., and Jesuthasan, S. J., "A microfluidic device to sort cells based on dynamic response to a stimulus," PLoS One **8**(11), e78261 (2013).
Tharmalingam, T., Ghebeh, H., Wuerz, T., and Butler, M., "Pluronic enhances the robustness and reduces the cell attachment of mammalian cells," Mol. Biotechnol. **39**(2), 167–177 (2008).
Toepfner, N., Herold, C., Otto, O., Rosendahl, P., Jacobi, A., Krater, M., Stachele, J., Menschner, L., Herbig, M., Ciuffreda, L., Ranford-Cartwright, L., Grzybek, M., Coskun, U., Reithuber, E., Garriss, G., Mellroth, P., Henriques-Normark, B., Tregay, N., Suttorp, M., Bornhauser, M., Chilvers, E. R., Berner, R., and Guck, J., "Detection of human disease conditions by single-cell morpho-rheological phenotyping of blood," Elife **7**, e29213 (2018).
Tsai, M. A., Waugh, R. E., and Keng, P. C., "Cell cycle-dependence of HL-60 cell deformability," Biophys. J. **70**(4), 2023–2029 (1996).
Walther, C. G., Whitfield, R., and James, D. C., "Importance of interaction between integrin and actin cytoskeleton in suspension adaptation of CHO cells," Appl. Biochem. Biotechnol. **178**(7), 1286–1302 (2016).
Wang, N., Butler, Jp Fau-Ingber, D. E., and Ingber, D. E., "Mechanotransduction across the cell surface and through the cytoskeleton," Science **260**(5111), 1124–1127 (1993).

Wang, X., Zhou, J., and Papautsky, I., "Vortex-aided inertial microfluidic device for continuous particle separation with high size-selectivity, efficiency, and purity," Biomicrofluidics **7**(4), e044119 (2013).
Wong, I. and Ho, C.-M., "Surface molecular property modifications for poly(dimethylsiloxane) (PDMS) based microfluidic devices," Microfluid. Nanofluid. **7**(3), 291–306 (2009).
Wu, G., Majewski, J., Ege, C., Kjaer, K., Weygand, M. J., and Lee, K. Y., "Lipid corralling and poloxamer squeeze-out in membranes," Phys. Rev. Lett. **93**(2), 028101 (2004).
Xavier, M., Rosendahl, P., Herbig, M., Krater, M., Spencer, D., Bornhauser, M., Oreffo, R. O., Morgan, H., Guck, J., andOtto, O., "Mechanical phenotyping of primary human skeletal stem cells in heterogeneous populations by real-time deformability cytometry," Integr. Biol. **8**(5), 616–623 (2016).
Xu, Z., Zheng, Y., Wang, X., Shehata, N., Wang, C., Xie, S., and Sun, Y., "Stiffening of sickle cell trait red blood cells under simulated strenuous exercise conditions," Microsyst. Nanoeng. **2**, 16061 (2016).
Yamada, M., Nakashima, M., and Seki, M., "Pinched flow fractionation: Continuous size separation of particles utilizing a laminar flow profile in a pinched microchannel," Anal. Chem. **76**(18), 5465–5471 (2004).
Yoon, Y., Kim, S., Lee, J., Choi, J., Kim, R.-K., Lee, S.-J., Sul, O., and S.-B. Lee, "Clogging-free microfluidics for continuous size-based separation of microparticles," Sci. Rep. **6**, 26531 (2016).